CEAS Space Journal
https://doi.org/10.1007/s12567-024-00562-y

ORIGINAL PAPER

Development of ultra-high temperature ceramic matrix composites for hypersonic applications via reactive melt infiltration and mechanical testing under high temperature

Luis Baier[1] · Martin Frieß[1] · Nils Hensch[1] · Vito Leisner[2]

Received: 27 June 2024 / Revised: 8 August 2024 / Accepted: 8 August 2024

Abstract
In the ongoing development of hypersonic technologies, material advancements play a key role in meeting the ever-increasing thermomechanical demands of these applications. Ultra-High Temperature Ceramic Matrix Composites (UHTCMCs) offer a promising solution for components operating under such extreme conditions. Their outstanding thermomechanical properties, including high temperature and thermal shock resistance, excellent thermal conductivity and mechanical strength, position them as ideal candidates for applications in fields like leading edges or inlet ramps for ramjets and scramjets. Due to their remarkable material composition, UHTCMCs are capable of operating in temperature regimes that surpass 1700 °C during their operation times under oxidizing atmospheres. At the German Aerospace Center (DLR), a UHTCMC material based on carbon fibres and a zirconium diboride matrix is being developed utilizing Reactive Melt Infiltration (RMI). With RMI, the orientation of the reinforcement fibres can be tailored, to enable the material to fulfill the demanding load requirements. The reactive melt infiltration process comprises three stages: preform fabrication, pyrolysis, and the actual melt infiltration. The foundation for important material properties of the final ceramic, including the matrix composition, is established in the preform production, which is a crucial step in the process. A boron- and zirconium diboride-based slurry is infiltrated into pitch-based carbon fibre fabric. Subsequently, the preforms are consolidated, pyrolysed, and infiltrated with molten Zr_2Cu to obtain the UHTC matrix by in situ reaction with the preform elements. Scanning Electron Microscopy (SEM) and Energy-dispersive X-Ray Spectroscopy (EDX) enable the examination of the microstructural features, including the arrangement and distribution of zirconium diboride within the matrix. Mechanical evaluation of the UHTCMCs is conducted via 3-point bending tests at both room temperature and at elevated temperature at 900 °C. It has been demonstrated that Ultra-High Temperature Ceramic Matrix Composites can be produced by means of reactive melt infiltration, and that they retain their strength even at elevated temperatures.

Keywords Ultra-high temperature ceramic matrix composite · Ceramic matrix composite · Ultra-high temperature ceramics · Carbon fibres · Zirconium diboride-based slurry · Reactive melt infiltration · Zr_2Cu · Mechanical testing

✉ Luis Baier
Luis.Baier@dlr.de

Martin Frieß
Martin.Friess@dlr.de

Nils Hensch
Nils.Hensch@dlr.de

Vito Leisner
Vito.Leisner@dlr.de

[1] Ceramic Composites and Structures, Institute of Structures and Design, German Aerospace Center (DLR), Pfaffenwaldring 38-40, 70569 Stuttgart, Germany

[2] Structural & Functional Ceramics, Institute of Materials Research, German Aerospace Center (DLR), Linder Höhe, 51147 Cologne, Germany

Abbreviations

C/C	Carbon Carbon
C/SiC	Carbon fibre-reinforced silicon carbide
C/HfB_2	Carbon fibre-reinforced hafnium diboride
C/ZrB_2	Carbon fibre-reinforced zirconium diboride
CMC	Ceramic Matrix Composite
DLR	German Aerospace Center
EDX	Energy dispersive X-ray spectroscopy
HfB_2	Hafnium diboride
RMI	Reactive melt infiltration
SEM	Scanning electron microscope
SiC/SiC	Silicon carbide fibre reinforced silicon carbide
UHTC	Ultra-High Temperature Ceramic

Published online: 19 August 2024

UHTCMC	Ultra-High Temperature Ceramic Matrix Composite
F	Fibre
M	Matrix

1 Introduction

The applications of hypersonic technology in the speed range above Mach 5 has recently been a steadily growing field in the aerospace industry, especially in the areas of re-entry vehicles and cruise missiles [1]. The requirements are defined by trajectories at low altitudes and thus in an oxidative atmosphere with flight times of less than one hour. In addition, these vehicles aim to be maneuverable. For aerodynamic reasons, sharp-edged geometries with small nose radii are preferred for these hypersonic vehicles, as they offer higher Lift-over-Drag ratios which improve maneuverability. These geometries in turn lead to extremely high heat loads occurring at the edges, as the heat flux increases inversely proportional to the nose radius and can reach a value of several 10^2 MW/mm^2, which can lead to temperatures in excess of 2000 °C [2–4]. For this reason, in the ongoing development of hypersonic technologies, material advancements play a key role in meeting the ever-increasing thermomechanical demands of these applications. For years, Ceramic Matrix Composite (CMC) materials have offered increasingly exciting possibilities to replace conventional metallic material classes and even surpass them in terms of characteristic values, because of their high mechanical values with comparably low densities at the same time. The aerospace and energy sectors in particular benefit from this, as the use of CMCs allows structures exposed to high thermal loads to be lighter, more durable or with improved efficiency [5]. Classic representatives of CMCs are primarily carbon–carbon (C/C), carbon fibre reinforced silicon carbide (C/SiC) and silicon carbide fibre reinforced silicon carbide (SiC/SiC). However, the disadvantage of all these materials is their use at elevated temperatures under atmospheric conditions. The erosion and oxidation of carbon-based materials already start at around 400 °C, SiC/SiC materials on the other hand lose their application possibilities from about 1600 °C due to active oxidation of the silicon-containing phases [6–8]. This disqualifies these materials, without complex active cooling, for certain applications in re-entry bodies, wing leading edges, scramjet and ramjet engines and generally structures in hypersonics where operating temperatures of over 1700 °C can be reached [2, 9]. Instead, the group of Ultra-High Temperature Ceramics (UHTCs) can be used. These are usually chemical binary compounds (borides, nitrides, carbides and oxides) of refractory metals, which are known for their high melting temperatures, usually far above 3000 °C, their operating temperatures above 2000 °C, as well as their resistance to erosion and oxidation. Examples for UHTCs are zirconium diboride (ZrB_2), zirconium carbide (ZrC), hafnium diboride (HfB_2) or titanium diboride [10, 11]. However, since these ceramics behave intrinsically brittle, the embedding of carbon or ceramic fibres in a UHTC matrix improves damage tolerance and thus a wide range of applications under high thermal and mechanical loads. This group of materials is called Ultra-High Temperature Ceramic Matrix Composites (UHTCMCs). Notable representatives are carbon fibre-reinforced zirconium diboride (C/ZrB_2) and carbon fibre-reinforced hafnium diboride (C/HfB_2) [12, 13]. Since UHTCMCs are a relatively new class of material—the first published papers date back to 2004—no real standardized process with a fully developed material for the production of UHTCMCs has yet been established.[14]. At the German Aerospace Center (DLR), a UHTCMC material based on carbon fibres and a zirconium diboride matrix is being developed utilizing a Reactive Melt Infiltration (RMI) process. Alongside chemical vapor infiltration, sintering and polymer infiltration & pyrolysis, the RMI process is one of the production routes for UHTCMCs [14]. The RMI process comprises three stages: preform fabrication, pyrolysis, and the actual melt infiltration. The process can be seen in Fig. 1 [15, 16].

The foundation for the material properties of the final ceramic, including the matrix composition, is established in the initial preform production, which therefore is a crucial step in the process. A boron- and zirconium diboride-based slurry is infiltrated into pitch-based carbon fibre fabric. The boron powder serves here as a reaction source for the subsequent infiltration with the zirconium melt, whereas the ZrB_2 serves as a supporting grain and is intended to partially absorb the exothermic reaction heat as an inert reaction participant. Subsequently of the powder infiltration, the preforms are consolidated with the assistance of a carbonaceous precursor, pyrolysed, and infiltrated with molten Zr_2Cu to obtain the UHTC matrix by in situ reaction with the preform elements. During pyrolysis, all volatile components of the preform are split off and a pore system forms within the matrix. Pyrolysis took place at 1300 °C for 30 min. During melt infiltration, the liquid zirconium-alloy melt infiltrates into this fine pore system due to the capillary forces and reacts with the preform elements in situ to form ZrB_2 and ZrC according to Eq. 1. A zirconium copper alloy is used to lower the melting point to allow infiltration at 1200 °C whereas an infiltration with pure zirconium would have to be at least above the melting point of Zr at a minimum of 1855 °C. to minimize degradation of the carbon fibres which occurs increasingly at higher temperatures. This low infiltration temperature helps to minimize the undesired reaction of the carbon fibres with the aggressive zirconium melt, as reactions take place more rapidly at higher temperatures.

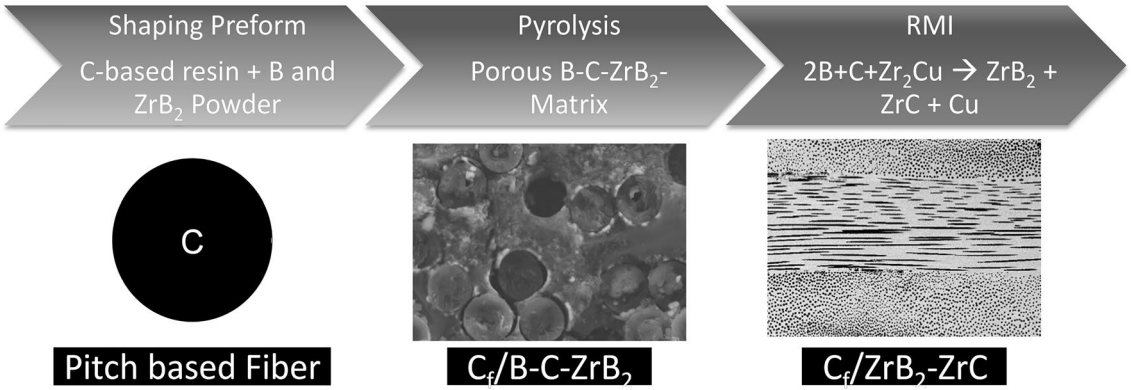

Fig. 1 RMI process route for the production of UHTCMCs, with images of the microstructure after pyrolysis and after RMI

$$\underbrace{C_F + B + ZrB_2 + C_M}_{\text{Preform}} + Zr_2Cu \xrightarrow{1200°C} C_F + ZrB_2 + ZrC + \text{Residual Melt} \quad (1)$$

The advantages of this process are near-net-shape production and short process times with inexpensive raw materials. Moreover, this process enables an embedding of the fibres into the component according to the actual load paths [17, 18]. At the current state of research, the most significant drawback is the relatively high proportion of unreacted residual melt within the UHTCMC matrix, as well as the still occurring degradation of fibre edge regions due to the highly reactive zirconium melt. For this reason, the current manufacturing process was further developed to increase the UHTC ratio of the matrix while reducing the amount of unreacted alloy at the same time and to understand property changes in the material under high-temperature conditions. For this purpose, mechanical behavior was investigated under room temperature and at elevated temperature conditions at 900 °C.

2 Methods and raw materials

As reinforcement material for the UHTCMC production, the pitch-based carbon fibre GRANOC XN-80-60S (Nippon Graphite Fibre Corporation, Japan) with a fibre diameter of 10 µm was used. A unidirectional fabric and a plain weave fabric are available for this fibre. In this study, the unidirectional fabrics were used. In the current production of UHTCMCs using RMI, the carbon fibre fabric is first infiltrated with a water-based slurry using a foulard. The slurry has a solids content of 50 wt%, which is made up of boron powder (25 wt%) and ZrB_2 powder (75 wt%). The amorphous boron powder for the slurry was supplied by Bayern Chemie GmbH (Germany). Zirconium diboride powder was provided by Höganäs (Sweden). A Partica LA-960 Laser Scattering Particle Size Distribution Analyzer (HORIBA Europe GmbH, Germany) was used to determine the particle sizes. A foulard from Mathis AG (Switzerland) was used to infiltrate the slurry into the fabric layers. The principle of a foulard consists of two counter-rotating rollers that apply pressure to each other. A slurry bath wets the fabric and the physical force of the rollers infiltrates the slurry into the fabric. This principle can be seen in Fig. 2 on the left. In the state-of-the-art process, both powders are used as supplied and are not treated. However, it was found, that slurry infiltration via foulard leads to inhomogeneous particle distribution throughout the preform, as can be seen in Fig. 2 on the right side. Here the ZrB_2 particles can be seen as white spots whereas boron powder cannot be seen due to the color contrasts, but as the particle size of the boron powder is equal or smaller than the ZrB_2 it can be assumed that the boron particles infiltrate slightly better into the fabrics. For the improved process the powders were ball-milled in isopropyl alcohol using a Pulverisette 6 planetary ball mill (Fritsch GmbH, Germany) before further processing into the slurry.

After infiltration, the fabric layers are dried, stacked and consolidated with the addition of a carbon-based precursor. A laboratory furnace from Diekmann GmbH (Germany) was used for the subsequent high-temperature steps of pyrolysis and melt infiltration process. The samples were then pyrolyzed at temperatures over 1200 °C to reduce the preform matrix to pure carbon, boron and ZrB_2. Finally, the preforms were melt infiltrated at 1200 °C for 3 min. For this purpose, the oven was equipped with a height-adjustable lifting device. For melt infiltration, the eutectic zirconium-copper alloy Zr_2Cu (HMW Hauner GmbH & Co. Kg) was selected. Copper was chosen as an alloying element to lower the melting temperature (pure Zr 1855 °C; Zr_2Cu 1002 °C) and hence minimize fibre degradation at melt infiltration. Microstructural analysis was performed using scanning electron microscopy (SEM) and energy-dispersive X-ray

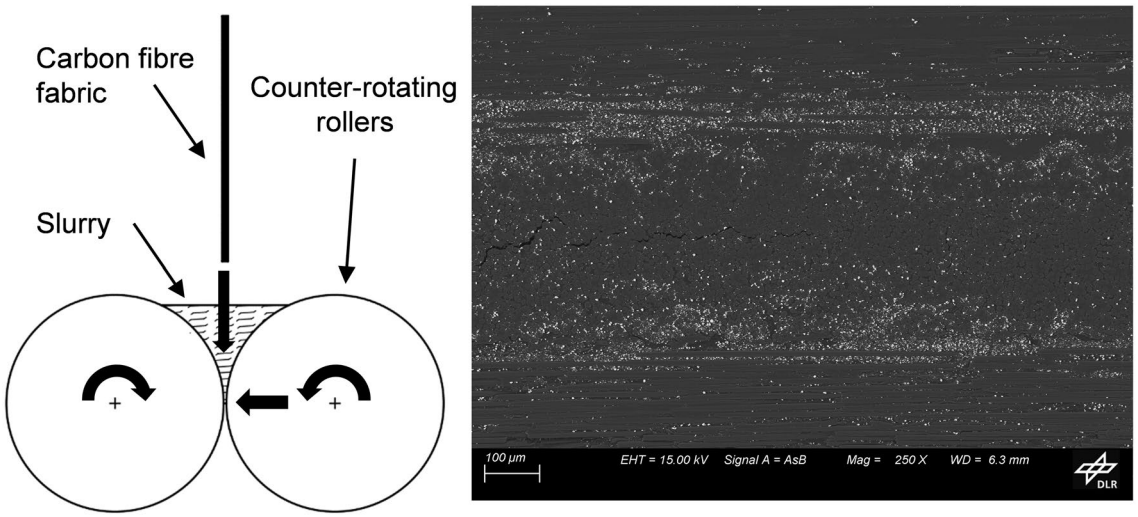

Fig. 2 Principle of slurry infiltration using a foulard (left); inhomogeneous particle distribution in the fibre rovings with initial slurry after infiltration – in white ZrB_2 powder (SEM picture 250×; right)

spectroscopy (EDX). A Zeiss GeminiSEM Ultra plus (Carl Zeiss AG, Germany) with an X-Max EDX Detector from Oxford Instruments (United Kingdom) was used for this purpose. All SEM pictures were taken using the angle-selective backscattered detector. ImageJ (Version 1.54f) was used to analyze the microstructures in terms of composition and UHTC contents by means of grayscale analysis. Mechanical evaluation of the UHTCMCs was conducted via 3-point bending tests at both room temperature and at elevated temperature based on the norm DIN EN 658-3. For room temperature tests a universal testing machine Zwick 1494 (ZwickRoell AG, Germany) was used. The DLR in-house Indutherm test machine was selected for the high-temperature tests, which was operated under vacuum (pressure < 1 mbar) to provide protection for the machine. Both machines were operated at a controlled crosshead speed of 1 mm/min and a support span of 50 mm. The bending strength was calculated from the maximum loads. Sample geometry for both test series was fixed at 60×10 x 2.5 mm^3. Room temperature samples were equipped with strain gauges to measure additional values. Microscope images were taken with a Keyence VHX-S550E digital microscope (Keyence, Japan) to evaluate the fracture behavior of the UHTCMC samples at room temperature and at elevated temperature. Density and porosity were determined according to the Archimedes method (DIN EN 993–1).

3 RMI development and mechanical testing

3.1 RMI development

This current RMI process is to be further developed with a focus on improving the matrix composition and lowering the residual melt phases. In this regard, particular attention is given to the initial slurry infiltration process in which the boron and ZrB_2 powders are infiltrated into the pitch-based carbon fibre fabrics. The goal is to achieve homogeneous infiltration with a high powder deposition into the fabrics down to the carbon fibre rovings, as Fig. 2 shows the currently inhomogeneous slurry infiltration into the carbon fabrics. To achieve a higher infiltration quality, either the slurry has to be improved or a new infiltration process can be developed, or a combination of both. The first step here is to adapt the slurry before adapting the process in the second step. The new slurry infiltration method investigated focuses on improving particle distribution and particle size to increase the UHTC matrix proportion throughout the composite and especially in the fibre bundles itself. As a first approach, the influence of the particle size of boron and ZrB_2 was investigated. First, the particle sizes of the received powder were measured. The amorphous boron powder had a d_{50} value (median particle size) of 2.03 µm and the zirconium diboride powder had a d_{50} value of 2.87 µm. Afterwards the maximum particle size with which infiltration into the fibre bundles is possible was determined. This maximum allowed particle size can be determined via the cavity size of the packing density of the fibres. A round cross-section can be assumed for carbon fibres. For the densest packing of

a fibre bundle, the densest circular packing with a maximum packing density of 0.907 can also be used for the most conservative approach. In conjunction with a fibre diameter of 10 µm, this results in a maximum particle size of 1.54 µm. As particles normally have an approximately normal distribution, the applied d_{50} value should be below 1 µm. Based on this the powders were ball milled up to 90 min in isopropyl alcohol. Isopropyl Alcohol was used to prevent unwanted reactions that could lead to the formation of hydrogen if, for example, water is used. To prevent the isopropyl alcohol from boiling, 10-min milling cycles were used and the milling chamber was cooled down in between. The resulting median particle sizes were $d_{50}=0.33$ µm for boron and $d_{50}=0.59$ µm for ZrB_2. Figure 3 shows the measured particle size distributions for boron and zirconium diboride powder as received and after ball milling. The relative distribution q [%] (shown in black) and the cumulative distribution Q [%] (shown in red) of the powders are plotted against the particle size in a logarithmic diagram. This clearly shows how milling appears to have an influence on coarse and fine particles, as the curves generally shift to the left towards finer particle sizes after milling. Both the maximum particle sizes and the smallest particle sizes decrease. The unground particles also appear to be partially agglomerated, which are measured here as particles larger than 10 µm.

To investigate the influence of the milled powders on the infiltration, carbon fibre fabrics were infiltrated with a ZrB_2 only slurry by a vacuum-assisted process and analyzed by means of SEM. Figure 4 shows the resulting SEM images (500×) with the received powder on the left and the ground powder on the right. It can be clearly seen that the ground powder infiltrates much better into the fibre bundle and leads to a significant increase in quantity and homogeneity. As the ground boron powder is even finer than the ZrB_2, it can be assumed that this effect is even more noticeable with the milled boron. The ground boron and ZrB_2 particles were

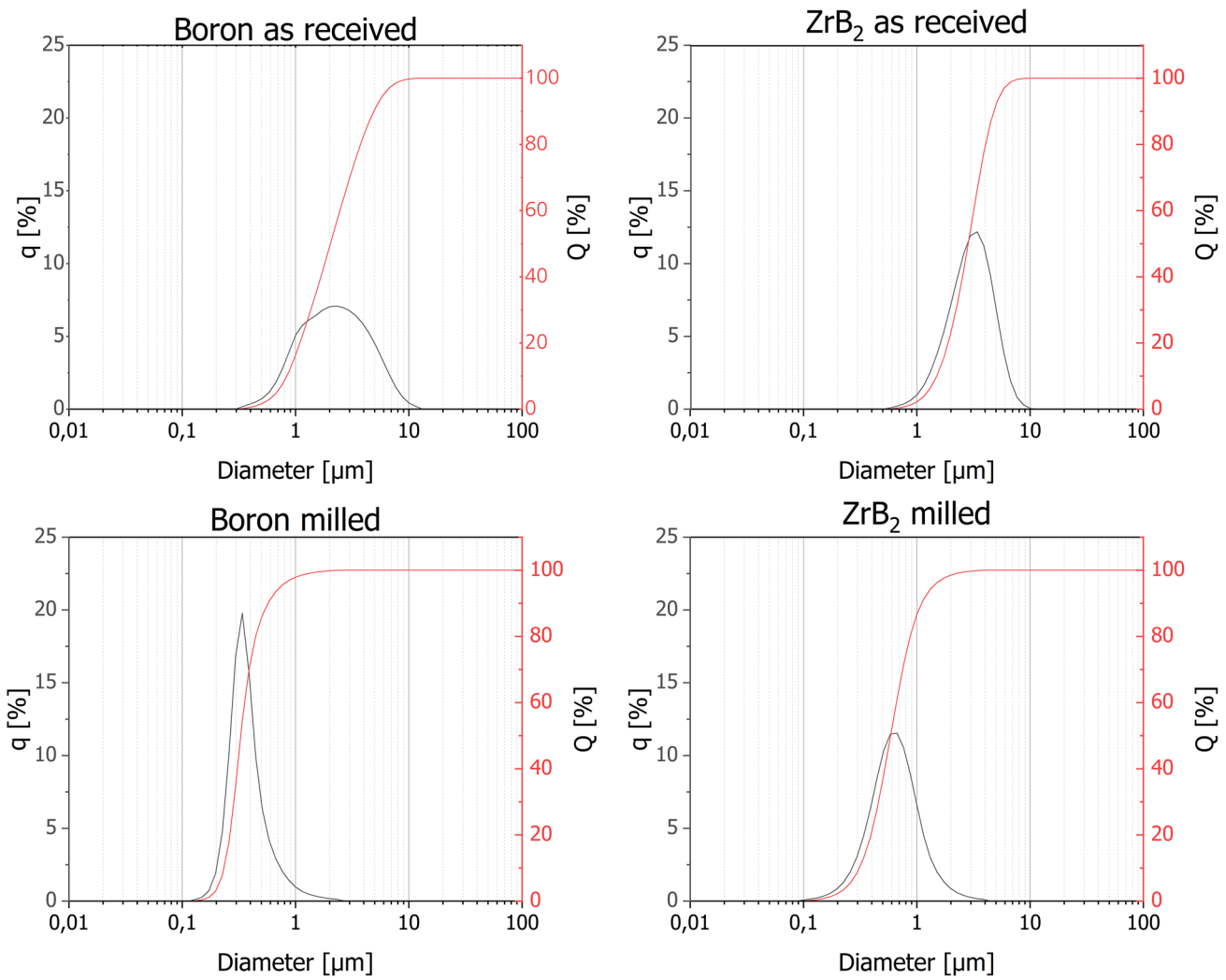

Fig. 3 Particle size distributions for boron and ZrB_2 as received and milled

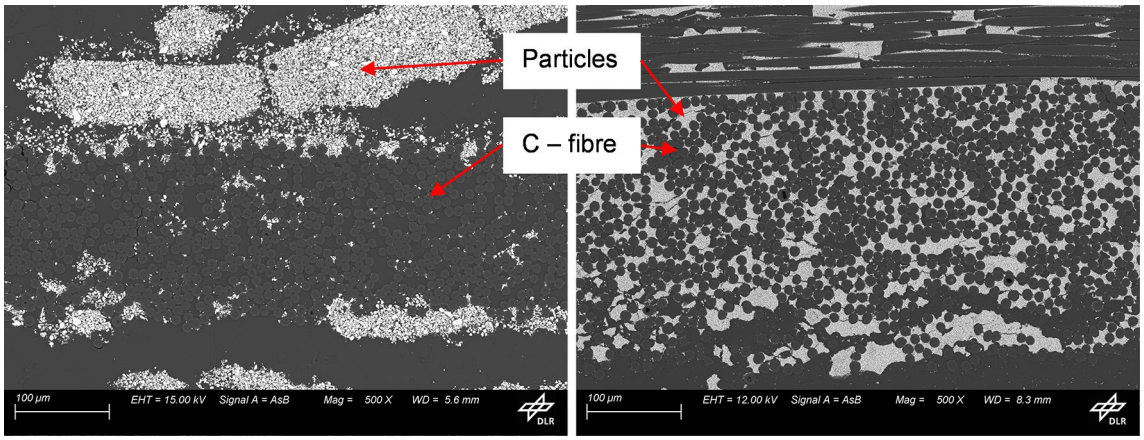

Fig. 4 Infiltration test with ZrB_2 only slurry with particles as received (left) and ground up (right); (SEM pictures 500×)

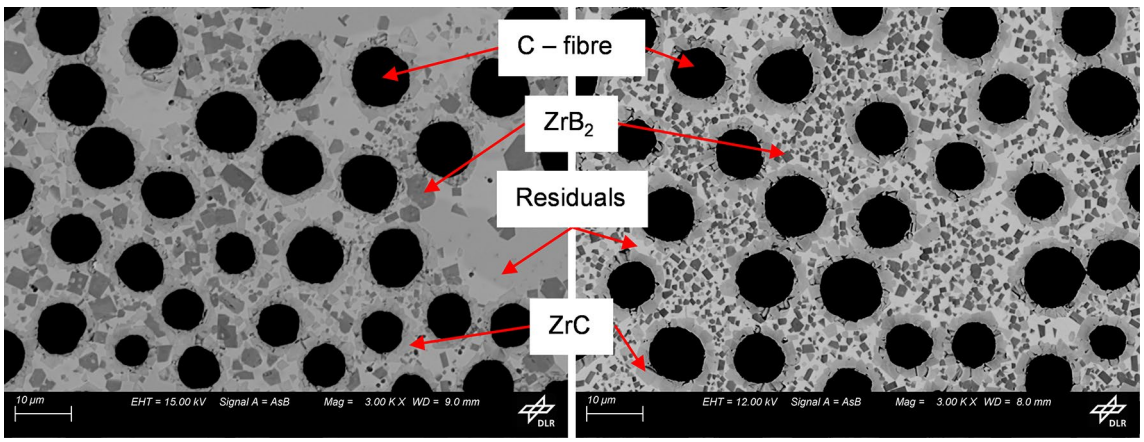

Fig. 5 Microstructure of reference UHTCMC material (left) and improved UHTCMC Material (right); (SEM pictures 3000×)

then used to produce a comparable slurry to the non-ground powder slurries, followed by fabric infiltration by foulard, drying and processing to UHTCMCs by melt infiltration. UHTCMCs manufactured according to the state-of-the-art process are hereinafter referred to as Reference material and samples with the milled powders as improved material.

3.2 Microstructural analysis

SEM and EDX enable examination of the microstructural features, including the arrangement and dispersion of zirconium diboride and zirconium carbide within the matrix. Zirconium carbide is mainly formed around the fibers due to the reaction between fibre and melt-in-melt infiltration. Figure 5 shows the microstructures for the reference material with as received powders on the left, as well as for the improved material with ground powders on the right, both at a magnification of 3000×. In these pictures, Carbon fibres are shown in black, zirconium diboride in dark grey, zirconium carbide

Table 1 Composition of the UHTCMCs

	C—Fibre (%)	UHTCs (%)	Residuals (%)
Reference UHTCMC Material	28.0	44.0	28.0
Improved UHTCMC Material	26.0	52.6	21.4

Table 2 Matrix-only Composition of the UHTCMCs

	UHTCs (%)	Residuals (%)
Reference Material	61.1	38.9
Improved Material	71.1	28.9

in grey and remaining melt in light grey. The percentages of composition for both UHTCMCs are shown in Table 1 each rounded to one decimal place. To compare the compositions of the matrices the Matrix-only compositions of the Composites were calculated by ImageJ and are shown in Table 2. A comparison of these two UHTCMCs shows directly that grinding the particles makes the ZrB_2 phases significantly smaller. However, this also means that the zirconium diboride is much more homogeneously distributed within the matrix as can be clearly seen in Fig. 5. In comparison, the reference sample shows larger areas in which the matrix consists only of residual melt without or with only a low UHTC content as can be seen in the SEM picture as well. In addition, grinding the base powders increases the overall UHTC content of the matrix from 61.1% for the reference sample up to 71.1% for the improved material due to this improved infiltrability, which means an increase of 16.4%. At the same time, this congruently reduces the amount of low-melting Zr–Cu residual phases in the matrix from 38.9 to 28.9%. For both materials, the fiber volume content is in a range between 25 and 30%.

Energy-dispersive X-ray spectroscopy was used to analyze the composition of the samples more precisely. In particular, the remaining copper content within the UHTCMCs was determined using EDX. Figure 6 shows the EDX distribution images for the elements zirconium, carbon and copper for an SEM image with 1000× magnification as well as the respective element distribution sum spectra for the reference material on the left and the improved material on the right, with values given in atomic percent. Boron is not recognized by the detector, as the boron peak is overlaid by the clearly pronounced carbon peak. For the reference material, the remaining copper content is 3.1 at%, whereas in the improved material sample, only 1.4 at% copper is present due to the increase in the ceramic phases, which reduces the residual melt content. This represents a decrease of 55%. Because of the low melting point of copper (1085 °C), minimizing the copper quantity inside the composite helps to increase the high-temperature properties of the ceramic. It can therefore be seen that grinding the source powders improves the homogeneity of the UHTC matrix and increases the overall UHTC content of the matrix while

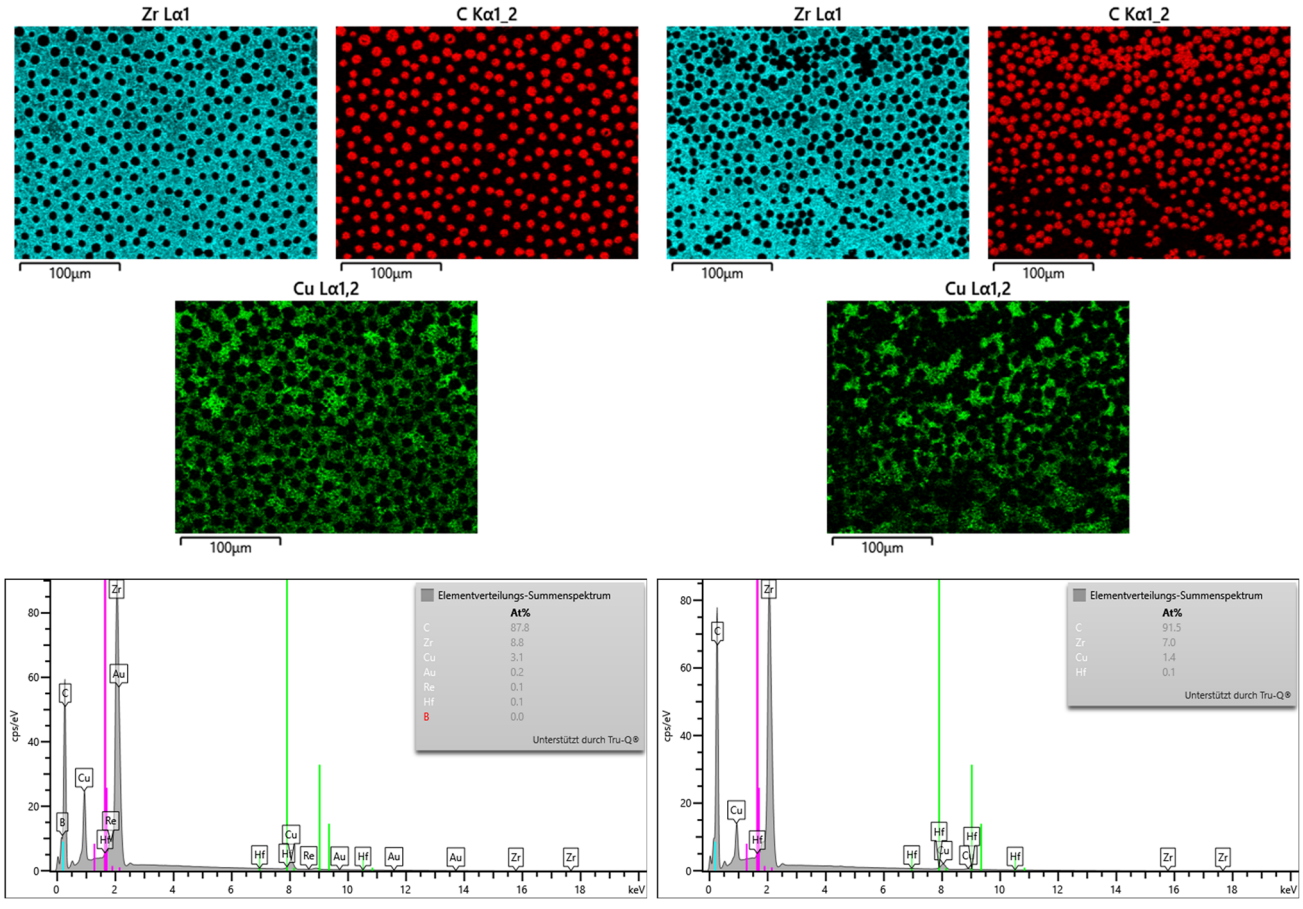

Fig. 6 EDX distribution images for zirconium, carbon and copper and EDX sum spectra for the reference sample (left) and improved sample (right)

Table 3 Mechanical values of Reference UHTCMC at room temperature (25 °C)

	Bending strength (MPa)	Young's modulus (GPa)	Elongation at break (%)
Mean Value	165.25	165.35	0.14
Standard Deviation	56.26	23.30	0.08

Table 4 Mechanical values of improved UHTCMC at room temperature (25 °C)

	Bending strength (MPa)	Young's modulus (GPa)	Elongation at break (%)
Mean Value	312.90	129.53	0.38
Standard Deviation	55.22	9.38	0.10

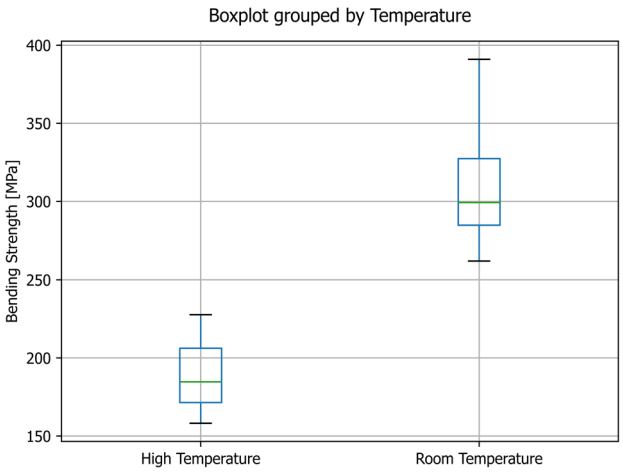

Fig. 7 Boxplots of the results of the 3-point bending test for room temperature and 900 °C for the improved UHTCMC material

lowering the residual copper content. Although the copper content could be reduced, copper still remains in the sample.

3.3 Mechanical testing

Finally, 3-point bending tests were performed on UHTCMC samples. Room temperature tests were carried out for both the reference material and the improved material. The improved material was also tested at 900 °C. These high-temperature tests were carried out under vacuum to protect the test bench. Tables 3 and 4 show the mechanical properties generated by 3-point bending at room temperature with the corresponding standard deviations both for the reference material in Table 3 and for the improved material in Table 4. For the reference material, the mean bending strength was 165.25 MPa, the young's modulus was 165.35 GPa and the elongation at break was 0.14%. The improved material, on the other hand, achieved a mean bending strength of 312.90 MPa at an elongation at break of 0.38% with a young's modulus of 129.53 GPa. This means an increase in bending strength of 89.35%, an increase in elongation at break of 171.45% and a decrease in the young's modulus of 21.66%. Thus, the desired quasi-ductile behavior of the material could be improved by a higher elastic deformation. At 900 °C, on the other hand, an average bending strength of 190.19 MPa with a standard deviation of 35.08 MPa was reached for the improved material. This corresponds to 60.78% of the bending strength at room temperature. The quite high standard deviations can occur due to the small number of samples of five per test series.

For better visualization of the improved material values and a good estimation of the distribution of the individual measured values, Fig. 7 shows the boxplots for the 3-point bending at 900 °C and room temperature. These are based on the same values for the improved material that were discussed before. The green line shows the median value of the bending strengths. The lower blue line is named the lower quartile, as the upper one is named the upper quartile. Between these two values, in the box, 50% of the measured values are distributed. For the whiskers, the upper and lower ends of the lines outside the boxes, the highest and lowest measured values were used here. The overall decrease in strength with increasing temperature can be explained primarily by the softening of the Zr-Cu residual phases, that were clearly visible in Fig. 6. The corresponding binary phase diagram of this system shows the first melting phases already from a temperature of 920 °C. A further reduction in the residual phases should therefore be able to further increase the high-temperature strengths. In addition, increasing the fibre volume content (currently quite low < 30%, compare Table 1) should increase the general strength over the entire temperature range.

Figure 8 shows examples of two 3-point bending specimens in cross-section after testing at 25 °C (left) and 900 °C (right) at a magnification of 100x. The matrix cracks caused by the tests can be clearly recognized in both samples. These images clearly show that, in contrast to a typical fracture of a monolithic ceramic, there is no brittle fracture behavior at either room temperature or at 900 °C. Instead, the crack deflection effect can be observed: the crack does not run straight through the specimen once being initiated but is repeatedly deflected at fibre bundles. Furthermore, none of the samples showed a complete fracture, and thus a catastrophic failure, which indicates a certain damage tolerance of the material both at room temperature and at 900 °C, which is typical for a ceramic matrix composite. However, both cross-sections show pores, as can be seen in Fig. 8. These pores are caused by insufficient infiltration with zirconium melt and reduce the mechanical properties as failure

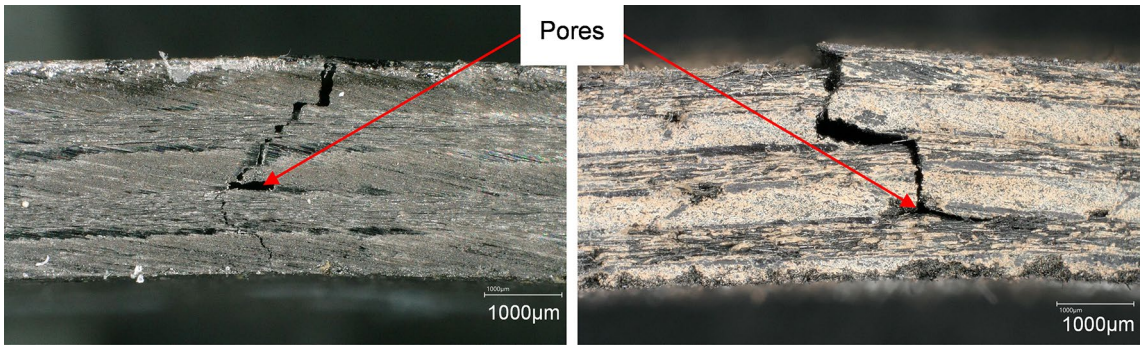

Fig. 8 Cross-sections of 3-point bending specimens after testing at 25 °C (left) and 900 °C (right) at 100×

Table 5 Density and Porosity of the improved UHTCMCs

	Density (g/cm^3)	Porosity (%)
Mean value	5.27	6.07
Standard deviation	0.26	2.17

often starts to develop at these defects. It can also be seen that the resulting cracks were probably initiated in the area of pores. By reducing the porosity in the future, it should be possible to further increase the mechanical properties accordingly. With reference to this, Table 5 shows the values for density and porosity for the 3-point bending samples as well as the corresponding standard deviations. The density is 5.27 g/cm^3. Due to the light carbon fibres (density 2.17 g/cm^3), this material is, therefore, lighter than the relevant matrix elements ZrB_2 (6.08 g/cm^3.), ZrC (6,73 g/cm^3.) and Zr-Cu (6.50—8.96 g/cm^3.). The porosity of 6.07% is a relatively high value for ceramics produced by reactive melting processes, where low porosities of less than 5% can normally be achieved. One reason for this is certainly the unidirectional fabric, which has a stabilizing weft fibre made of a polymer that burns out during pyrolysis and leaves behind pores that cannot be filled with the melt by capillary forces. In the future, a different type of weave could be used to minimize the formation of this porosity.

4 Conclusion

Due to their material characteristics, the class of UHTCMCs offers the potential for use in hypersonic vehicles, for structural components exposed to high thermomechanical loads. Zirconium diboride-based materials are particularly interesting due to their high-temperature stability. DLR is therefore developing a carbon fibre-reinforced ZrB_2.

It has been demonstrated that Ultra-High Temperature Ceramic Matrix Composites based on zirconium diboride and zirconium carbide can be produced by means of a reactive melt infiltration process and, that by adapting the used slurry at the preform production process, an improved particle infiltration could be achieved. This led to an overall increase of the UHTC content by 16,4% and a better, more homogeneous distribution inside of the composite matrix, especially with regard to zirconium diboride. At the same time, the proportion of low-melting copper was reduced by almost 55% to 1.4 at%. Low-melting copper phases are a major cause of temperature limitation of UHTCMCs produced by means of reactive melt infiltration and should therefore be minimized.

Mechanical characterization was carried out by means of three-point bending tests. For the improved UHTCMC material three-point bending tests at room temperature achieved an average bending strength of 312.90 MPa with an elongation at break of 0.38% and therefore improved the overall bending strength by nearly 90% in comparison to the reference material. At 900 °C, the flexural strength of the improved material decreased by 40% in comparison to the room temperature test to an average of 190.19 MPa. Both at room temperature and at elevated temperature, the UHTCMCs showed typical damage-resistant behavior. This test at 900 °C was intended to generate initial data on this material to better understand its behavior at this temperature. By further reducing the amount of copper, or by using a completely new alloy in the future, the high-temperature stability should be further investigated and increased.

Acknowledgements This paper is intended for the "HiSST Special Issue"

Author contribution L.B. wrote the main manuscript text and was mainly responsible for the experimental work, unless otherwise described M.F. provided fundamental input for all areas of the production process, especially at the chemical level and also revised also works critically for important intellectual content N.H was responsible for the evaluation of the mechanical characterization, in particular Tables 3, 4 and Fig. 7 V.L. made substantial contributions to the parts of the work dealing with powder milling, dispersion and slurry composition (Fig. 3). All authors reviewed the manuscript.

Funding Open Access funding enabled and organized by Projekt DEAL. Open access funding enabled and organized by Projekt DEAL.

Data availability No datasets were generated or analysed during the current study.

Declarations

Conflict of interest The authors declare no competing interests.

References

1. Millar, K. K., Brannon: The rise of hypersonics: hypersonic weapons and flight breaking new barriers – Überprüfungsdatum 2024–01–03
2. Glass, D.: Ceramic Matrix Composite (CMC) Thermal Protection Systems (TPS) and Hot Structures for Hypersonic Vehicles. In: 15th AIAA International Space Planes and Hypersonic Systems and Technologies Conference : American Institute of Aeronautics and Astronautics, 2008 (International Space Planes and Hypersonic Systems and Technologies Conferences).
3. Sziroczak, D., Smith, H.: A review of design issues specific to hypersonic flight vehicles. Prog. Aerosp. Sci. **84**, 1–28 (2016)
4. Wright, D., Tracy, C.: The physics and hype of hypersonic weapons: these novel missiles cannot live up to the grand promises made on their behalf, aerodynamics shows. Sci. Am. **325**, 64–71 (2021)
5. Roth, R., Clark, J.P., Field, F.R.: The potential for CMCs to replace superalloys in engine exhaust ducts. JOM **46**, 32–35 (1994)
6. Hülsenberg, D.: Keramik. Springer Vieweg, Berlin (2014)
7. Jacobson, N.S., Opila, E.J., Fox, D.S., Smialek, J.L.: Oxidation and corrosion of silicon-based ceramics and composites. Mater. Sci. Forum **251–254**, 817–832 (1997)
8. Gee, S.M., Little, J.A.: Oxidation behaviour and protection of carbon/carbon composites. J. Mater. Sci. **26**, 1093–1100 (1991)
9. Justin, J.F., Julian-Jankowiak, A., Guérineau, V., Mathivet, V., Debarre, A.: Ultra-high temperature ceramics developments for hypersonic applications. CEAS Aeronaut. J. **11**, 651–664 (2020)
10. Ionescu, E., Bernard, S., Lucas, R., Kroll, P., Ushakov, S., Navrotsky, A., Riedel, R.: Polymer-derived ultra-high temperature ceramics (UHTCs) and related materials. Adv. Eng. Mater. **21**(8), 1900269 (2019)
11. Wuchina, E., Opila, E., Opeka, M., Fahrenholtz, B., Talmy, I.: UHTCs: ultra-high temperature ceramic materials for extreme environment applications. Electrochem. Soc. Interface **16**(4), 30–36 (2007)
12. Paul, A., Jayaseelan, D. D., Venugopal, S., Zapata-Solvas, E., Binner, J. G. P., Vaidhyanathan, B., Heaton, A., Brown, P. M., Lee, W. E.,: UHTC composites for hypersonic applications (2012)
13. Tang, S., Hu, C.: Design, preparation and properties of carbon fiber reinforced ultra-high temperature ceramic composites for aerospace applications: a review. J. Mater. Sci. Technol. (2016). https://doi.org/10.1016/j.jmst.2016.08.004
14. Rueschhoff, L.M., Carney, C.M., Apostolov, Z.D., Cinibulk, M.K.: Processing of fiber-reinforced ultra-high temperature ceramic composites: a review. Int. J. Ceramic Eng. Sci. **2**(2), 22–37 (2020)
15. Kütemeyer, M., Schomer, L., Helmreich, T., Rosiwal, S., Koch, D.: Fabrication of ultra high temperature ceramic matrix composites using a reactive melt infiltration process. J. the European Ceram. Soc. **36**(15), 3647–3655 (2016)
16. Kütemeyer, M., Helmreich, T., Rosiwal, S., Koch, D.: Influence of zirconium-based alloys on manufacturing and mechanical properties of ultra high temperature ceramic matrix composites. Adv. Appl. Ceram. **117**, s62–s69 (2018)
17. Kütemeyer, M.: Development of Ultra High Temperature Matrix Composites using a Reactive Melt Infiltration Process. Karlsruher Institut für Technologie (KIT). Ph.D. thesis. 2021
18. Rubio, V., Ramanujam, P., Binner, J.: Ultra-high temperature ceramic composite. Adv. Appl. Ceram. **117**, s56–s61 (2018)